fes S_L probe are seen to correspond. Similarly, correspondence was observed between v-*fes* S_R homologous restriction fragments as determined by genomic blots of total cellular DNA and the isolated human homolog of the GA/ST v-*fes* gene. The human v-*fes* homolog showed no detectable transforming activity when transfected to RAT-2 cells by means of a thymidine kinase selection system. Molecularly cloned GA/ST FeSV were included as positive controls.

The molecular cloning of human genomic sequences homologous to GA/ST FeSV v-*fes* is of particular interest because (i) the c-*fes* gene is highly conserved and (ii) it is subject to frequent recombination with type C retrovirus sequences resulting in the generation of transforming viruses (*7, 9*). Virus isolates of this class of not only mammalian (feline) but also avian (chicken) origin contain related cellular derived transforming sequences (*10*). A common feature of the major gene product of these recombinant transforming viruses is an associated tyrosine-specific protein kinase (*11–13*). In addition, the GA and ST FeSV gene products exhibit binding affinity for a 150,000 molecular weight cellular phosphoprotein (*12, 14*) and transformation by these viruses leads to abolition of epidermal growth factor binding (*15, 16*) and production of a low molecular weight transforming growth factor (*17*).

The finding of only a single genetic locus exhibiting significant homology with the GA and ST FeSV acquired sequences establishes that the highly related transforming sequences within the genomes of these independently isolated viruses were originally derived from the same cellular gene. Conversely, molecular probes specific for acquired cellular sequences represented within the Abelson MuLV genome, an independent RNA transforming virus with associated protein kinase activity (*11, 18*), recognized different human DNA restriction fragments and lacked detectable homology with sequences represented within any of the three cosmid isolates (data not shown). Thus there must exist at least two independent loci within the human genome homologous to viral genes with associated tyrosine-specific protein kinase activities.

The human carcinoma DNA cosmid library generated in our study provides a specific reagent for the molecular cloning of cellular homologs of viral transforming genes. In particular, the availability of this library should be of value for the isolation of those human transforming genes with extensive intervening sequences. An important feature of this system is the presence of a functionally active thymidine kinase gene that allows for selection of minority populations of eukaryotic cells containing such cosmids after transfection. In addition, SV40 DNA sequences situated in one of the cosmid arms have been shown to exert a positive influence on transcription in the β-globin system (*6*). If this sequence similarly influences expression of cellular homologs of viral transforming genes, its presence may be important for identification of the translational products of these sequences and a determination of their transforming potential.

JOHN GROFFEN
NORA HEISTERKAMP
Laboratory of Viral Carcinogenesis, National Cancer Institute, Frederick, Maryland 21701
FRANK GROSVELD
Laboratory of Gene Structure and Expression, Medical Research, Council, London NW7 1AA
WIM VAN DE VEN
Carcinogenesis and Intramural Program, Frederick Cancer Research Facility, Frederick, Maryland 21701
J. R. STEPHENSON
Laboratory of Viral Carcinogenesis, National Cancer Institute, Frederick, Maryland 21701

References and Notes

1. P. J. Fischinger, in *Molecular Biology of RNA Tumor Viruses*, J. R. Stephenson, Ed. (Academic Press, New York, 1980), p. 162.
2. G. Franchini, J. Even, C. J. Sherr, F. Wong-Staal, *Nature (London)* **290**, 154 (1981).
3. S. P. Goff, E. Gilboa, O. N. Witte, D. Baltimore, *Cell* **22**, 777 (1980); R. Dalla-Favera, E. P. Gelmann, R. C. Gallo, F. Wong-Staal, *Nature (London)* **292**, 31 (1981); R. W. Ellis, D. DeFeo, T. Y. Shih, M. A. Gonda, H. A. Young, N. Tsuchida, D. R. Lowy, E. M. Scolnick, *ibid.*, p. 506; D. Shalloway, A. D. Zelenetz, G. M. Cooper, *Cell* **24**, 531 (1981).
4. D. Horowicz and J. F. Burke, *Nucl. Acids Res.* **9**, 2989 (1981).
5. F. G. Grosveld, H. M. Dahl, E. de Boer, R. A. Flavell, *Gene* **13**, 227 (1981).
6. F. Grosveld, T. Lund, A. Mellor, H. Bud, H. Bullman, R. A. Flavell, *J. Mol. Appl. Genet.*, in press.
7. L. A. Fedele, J. Even, C. F. Garon, L. Donner, C. J. Sherr, *Proc. Natl. Acad. Sci. U.S.A.* **78**, 4036 (1981).
8. E. M. Southern, *J. Mol. Biol.* **98**, 503 (1975).
9. M. A. Barbacid, A. V. Lauver, S. G. Devare, *J. Virol.* **33**, 196 (1980); W. J. M. Van de Ven, A. S. Khan, F. H. Reynolds, Jr., K. T. Mason, J. R. Stephenson, *ibid.* **33**, 1034 (1980).
10. M. Shibuya, T. Hanafusa, H. Hanafusa, J. R. Stephenson, *Proc. Natl. Acad. Sci. U.S.A.* **77**, 6536 (1980).
11. W. J. M. Van de Ven, F. H. Reynolds, Jr., J. R. Stephenson, *Virology* **101**, 185 (1980).
12. F. H. Reynolds, Jr., W. J. M. Van de Ven, J. R. Stephenson, *J. Biol. Chem.* **255**, 11040 (1980).
13. M. Barbacid, K. Beemon, S. G. Devare, *Proc. Natl. Acad. Sci. U.S.A.* **77**, 5158 (1980).
14. F. H. Reynolds, Jr., W. J. M. Van de Ven, J. R. Stephenson, *Nature (London)* **286**, 409 (1980).
15. F. H. Reynolds, Jr., W. J. M. Van de Ven, J. Blomberg, J. R. Stephenson, *J. Virol.* **37**, 643 (1981).
16. G. J. Todaro, J. E. DeLarco, S. Cohen, *Nature (London)* **264**, 26 (1976).
17. J. R. Stephenson and G. J. Todaro, in *Advances in Viral Oncology*, G. Klein, Ed. (Raven Press, New York, in press), vol. 1.
18. O. N. Witte, A. Dasgupta, D. Baltimore, *Nature (London)* **283**, 826 (1980); J. Blomberg *et al.*, *ibid.* **286**, 504 (1980).
19. R. Bernards and R. A. Flavell, *Nucl. Acids Res.* **8**, 1521 (1980).

20. We thank R. A. Flavell for advice and discussion, C. J. Sherr for providing plasmids containing the S_R v-*fes* and S_L v-*fes* subclones, and G. T. Blennerhassett and P. Hansen for technical assistance. Supported under Public Health Service Contract No. NOI-CO-75380 from the National Cancer Institute, by the British Medical Research Council (MRC), and by a grant (NUKC-BIOCH 80-1) awarded to J.G., N.H., and W.V.D.V. by the Royal Netherlands Cancer Foundation (KWF).

18 January 1982; revised 22 March 1982

Variables on Scatterplots Look More Highly Correlated When the Scales Are Increased

Abstract. *Judged association between two variables represented on scatterplots increased when the scales on the horizontal and vertical axes were simultaneously increased so that the size of the point cloud within the frame of the plot decreased. Judged association was very different from the correlation coefficient,* r, *which is the most widely used measure of association.*

Graphs are mainstays of the analysis and presentation of scientific data. One reason is that numerical summaries cannot always portray data unambiguously. For example, the most common measure of the association, or relation, between two variables $(x_i y_i)$, $i = 1, \ldots, n$, is the absolute value of the correlation coefficient, r, which measures the linear association between two variables (*1*). When there is no linear association, $|r|$ is 0; when there is perfect linear association so that x_i and y_i lie along a straight line, $|r|$ is 1. However, different configurations of points can yield the same value of r, relations can be nonlinear, and a single value of (x_i,y_i) can radically alter r (*2*). A scatterplot can depict the relation between x_i and y_i more reliably than any single numerical measure. But the use of a graph opens the door for perceptual factors to enter into the analysis and interpretation of the data. Although a set of data has only one numerical value for a particular measure of association such as r, the judged association could change according to any one of a number of "display factors" such as the size of the

0036-8075/82/0604-1138$01.00/0

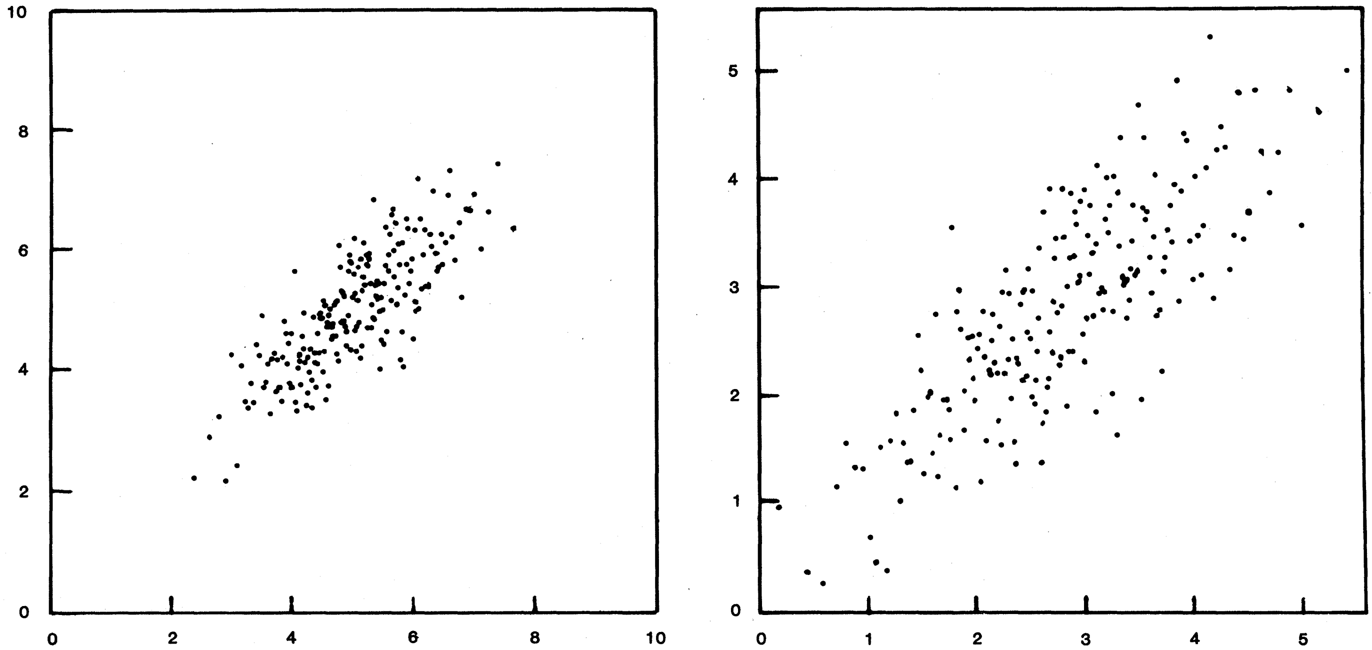

Fig. 1. Reductions of two scatterplots used in the three types of experiments. The left panel is point-cloud size 2 and the right panel is point-cloud size 4. In both panels $w(r) = .4$ and $r = .8$.

plotting character, the overall size of the display, the orientation of the point cloud within the frame, and the size of the point cloud within the frame. The last two factors are controlled by the scales of the vertical and horizontal axes in graphs with a plotting area of fixed size.

To investigate how people judge association from scatterplots and how display factors affect their judgments, we did three experiments. Our subjects consisted of students in university courses in statistics, university faculty members in statistics and mathematics, and practicing statisticians in government and industry.

In the first experiment, 74 subjects viewed 19 scatterplots, all with 0 or positive correlation coefficients. The subjects were asked to judge linear association on a scale from 0 (no linear association) to 100 (perfect linear association). The scatterplots in Fig. 1 are reductions of two of the stimuli from this experiment; the reader is invited to judge the association on these plots in order to understand the nature of the judgment task (*3*).

We varied two factors: amount of association and point-cloud size. The size of the frame was kept fixed. There were ten levels of association; each scatterplot had a value of $w(r) = 1 - \sqrt{1 - r^2}$ equal to one of the values 0, .05, .1, .2, . . . , .8, $w(r)$ being another numerical measure of linear association that goes from 0 to 1 as r goes from 0 to 1. An interpretation of $w(r)$ in terms of the geometry of the point cloud will be given later; we used $w(r)$ because it seemed, a priori, closer to people's subjective scales than r. There were four point-cloud sizes; they are labeled 1 to 4, size 1 being the smallest and size 4 the largest. For point-cloud size 3 there were ten scatterplots with the ten different values of $w(r)$, and for each of the other sizes there were three scatterplots with values of $w(r)$ equal to .1, .4, and .7.

Each scatterplot had 200 points and a square frame with sides equal to 17.3 cm. In all cases the center of gravity of the point cloud was at the center of the frame. The values portrayed on the horizontal axis of the kth scatterplot, $x_i(k)$, for $i = 1, \ldots, 200$, and the values portrayed on the vertical axis, $y_i(k)$, for $i = 1, \ldots, 200$, formed a bivariate supernormal point cloud (*4*) which ensured highly regular behavior: a linear relation, no peculiar points, and an elliptical appearance. The major axis of each point cloud was the line $y = x$ and the minor axis was the line $y = -x$.

The minimum value portrayed on the two axes of all plots was 0 data units and the maximum value was 5.6, 7, 10, or 14 data units. The length of each axis was 17.3 cm; the four scale values were therefore .32, .40, .58, and .81 data units per centimeter. The effect of decreasing the scale was to increase the size of the point cloud within the frame.

There were four orders of presentation of the 19 scatterplots with approximately one-fourth of the subjects judging each order. Two of the orders were random and the other two were the reverses of those.

The scatterplots were presented in stapled booklets with 8½ by 11 inch pages. First there were written instructions and sample scatterplots, then four trial plots that subjects judged; no feedback was given. Finally, there were the 19 experimental plots, each on a separate page. The subjects were asked to give their own subjective assessment of the amount of linear association, rather than to judge the correlation coefficient, and were asked not to look back or change old answers. It was suggested that they work reasonably quickly and that most people could comfortably make a single judgment within 15 seconds.

Our data analyses made extensive use of 10 percent trimmed means (*5*), which are defined in the following way: Order the observations from smallest to largest; drop the largest 10 percent of the observations and the smallest 10 percent; take the arithmetic average of the remaining values. Ten percent trimmed means are robust estimates (*6*) because they are not distorted by a small fraction of outliers, and they are a compromise between arithmetic means, which are 0 percent trimmed means, and medians, which are trimmed means close to the 50 percent level. The standard errors of 10 percent trimmed means can be computed from a formula given in (*7*).

Judged association for each of the 19 scatterplots was summarized by 10 percent trimmed means of the subjects' guesses divided by 100 (*8*). These values are plotted in Fig. 2 against the actual values of r for the 19 scatterplots; also portrayed are the standard errors of the trimmed means (*9*). The two curves are

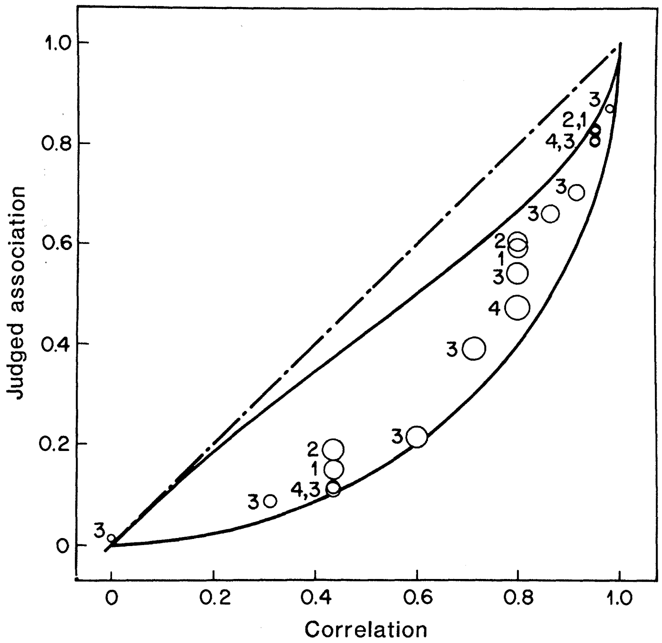

Fig. 2. The 10 percent trimmed means across subjects of judged association divided by 100 for 19 scatterplots are plotted (by the circle centers) against the values of r, the correlation coefficient, of the scatterplots. The circle radii portray the standard errors of the trimmed means. Thus the circle areas are proportional to the estimated variances of the trimmed means. The numbers to the left of the circles indicate the point-cloud sizes. When two numbers are shown, separated by a comma, two circles are nearly coincident and the first number refers to the circle with the smaller trimmed mean. The upper solid curve on the plot is $g(r)$ and the lower solid curve is $w(r)$. The dashed line is the line $y = x$. The information on the plot leads to two conclusions: judged association tends to increase as the point-cloud size decreases because of increasing scale; judged association is very different from the standard numerical measure of association, the correlation coefficient.

$w(r)$ and $g(r) = 1 - \sqrt{(1 - r)/(1 + r)}$, $g(r)$ being another measure of linear association that goes from 0 to 1 as r goes from 0 to 1. An interpretation of $g(r)$ in terms of the geometry of the point cloud will be given later.

The judged association is seen to be quite different from the standard numerical measure, r, with 10 percent trimmed means well below the line $y = x$. This result has been found in two other experiments (*10*) in which subjects were asked to guess the correlation coefficient from scatterplots and in experiments in which the amount of association was judged on the basis of other kinds of stimuli (*11*). [Two related but not directly relevant experiments are reported in (*12*) and (*13*).] Interestingly, these results also correspond to a statement by Wilk (*14*): ". . . it is felt by some [applied statisticians] that values of $|r|$ below .5 are quite 'small', while r is 'large' only when $|r|$ is above .8, and r is 'really large' (close to a linear dependence of the variables) only when $|r|$ is above .95." Wilk argues that $w(r)$ is a more sensible numerical measure of association than r; Fig. 2 shows that $w(r)$ does come closer to describing the perceived association for our subjects than does r.

The tendency is for judged association to increase as the point-cloud size is decreased by the increase in the scales; the effect is most pronounced when $w(r) = .4$. In all cases the perceived associations for sizes 1 and 2 are greater than those for sizes 3 and 4. The effect, however, does not appear to extend beyond size 2: for all three values of $w(r)$, the trimmed mean for point-cloud size 2 is either very close to that of size 1 or somewhat greater, and sizes 3 and 4 differ from one another by a nontrivial amount only for $w(r) = .4$ ($r = .8$).

To investigate the statistical significance of the effect of changing scale we performed the following operations: For each subject and each level of $w(r)$ in which scale was varied [$w(r) = .1, .4, .7$] we subtracted the subject's estimate for the largest point-cloud size, 4, from each of the estimates for the other three sizes, which for each subject yielded three differences for each of the three levels of $w(r)$; then we computed 10 percent trimmed means and their standard errors across the subjects. Each trimmed mean divided by its standard error has, approximately, a t distribution with 57 degrees of freedom (*7*); this distributional result can be used to test the significance of the difference between the point-cloud size 4 response and the responses to each of the other sizes. For $w(r) = .1$ the size 4 response is significantly different (at the .01 level) only from the size 2 response; for $w(r) = .4$ the size 4 response is significantly different from all three of the other responses; for $w(r) = .7$ the size 4 response is significantly different only from the size 1 response.

In the second experiment we checked this effect of scale under different conditions. We showed the two scatterplots in Fig. 1 alternatively, by an overhead transparency projected onto a screen in the front of a room, to 109 subjects in three groups of 27, 36, and 46 people. They were asked to assess the association of each plot on a scale of 0 to 100. The 10 percent trimmed mean of [(judgment for point-cloud size 2) − (judgment for point-cloud size 4)]/100 across subjects is .068 with a standard error of .011. The 10 percent trimmed mean of the corresponding values for the subjects in the first experiment is .125 with a standard error of .018.

In a third experiment 32 subjects in a single group were shown the scatterplots in Fig. 1 in the same manner as the subjects in the second experiment, but were told that the correlation coefficients of the two scatterplots were the same. They were asked to indicate whether one of the two "looked" more highly correlated than the other and if so, which one; 66 percent indicated that the size 2 scatterplot looked more correlated, 13 percent indicated the size 4 scatterplot, and 22 percent said they looked the same. This has the same pattern as in the first experiment, where the corresponding percentages are 81, 18, and 15, and in the second experiment, where the corresponding percentages are 59, 11, and 30.

Thus the second and third experiments strongly corroborate the conclusion of the first: increasing the scales on the horizontal and vertical axes of a scatterplot so as to decrease the point-cloud size increases the judged association.

Knowing what perceptual strategies people employ in judging association from scatterplots might not only provide an explanation of the effect of scale in our three experiments, but might also enable more effective design of scatterplots. The point clouds on the scatterplots in our experiments have an elliptical look because the bivariate normal distribution, from which we can think of the points as arising, has a density with elliptical contours. Two of the features of the point clouds are the ratio of the lengths of the minor and the major axes and the area. Subjects might be using either to judge association.

The ratio of the minor axis to the major axis of a contour of the associated bivariate normal distribution is $\sqrt{(1 - r)/(1 + r)}$, since the standard deviations of $x_i(k)$ and $y_i(k)$ are equal and the scales on the horizontal and vertical axes of each scatterplot are the same. If subjects were judging association by judging the ratio of the axes of the point cloud, then the judged scale would be $g(r)$, which, as described earlier, is shown in Fig. 2.

The area of an elliptical contour of the associated bivariate normal distribution divided by the area of a rectangle with sides parallel to the horizontal and vertical axes of the plot is equal to $.25\pi \sqrt{1 - r^2}$. If subjects were judging association by judging the areas of the point clouds relative to a circumscribed rectangle, the judged scale would be $w(r)$, which, as described earlier, is shown in Fig. 2.

Neither of the curves $w(r)$ and $g(r)$ appears to describe the judged association (*15*). It could be, however, that one of the two geometrical tasks—judging axis ratios or judging areas—is being carried out but that there are biases in the judgments that alter the perceived association. For example, it is known that judgments of area and length tend to be proportional not to the physical quantity but rather to the physical quantity to a power less than 1 (*16*). New experiments are needed in order to better understand the perceptual mechanism that people use in judging association (*17*).

WILLIAM S. CLEVELAND
Bell Laboratories,
Murray Hill, New Jersey 07974
PERSI DIACONIS
Stanford University,
Stanford, California 94305
ROBERT MCGILL
Bell Laboratories, Murray Hill

References and Notes

1. G. W. Snedecor and W. G. Cochran, *Statistical Methods* (Iowa State Univ. Press, Ames, 1967).
2. S. J. Devlin, R. Gnanadesikan, J. R. Kettenring, *Biometrika* **62**, 531 (1975); F. J. Anscombe, *Am. Stat.* **27**, 17 (1973).
3. The written instructions to subjects included: "This is an experiment to find out how people such as you assess the association of two variables from a scatterplot. We will measure association on a scale of 0 to 100. Zero means no association and 100 means perfect linear association" and "We are going to show you scatterplots and ask you to rate on a scale of 0 to 100 what your subjective assessment of the association is. There is no right answer. We are interested in what the association appears to be to you."
4. Let q_i for $i = 1, \ldots, 200$ be equally spaced quantiles of the normal distribution so that $\Phi(q_i) = (i - .5)/200$. Let u_i be the q_i divided by their standard error. The values portrayed on the horizontal axis of the kth scatterplot are $x_i(k) = \alpha(k) + \beta u_i$ for $i = 1, \ldots, 200$. Let $v_i(k)$ be a random permutation of the u_i; linearly regress $v_i(k)$ on u_i and let $w_i(k)$ be the residuals divided by their standard error. Let r_k be the desired correlation coefficient of the kth scatterplot. The values portrayed on the vertical axis of the plot are $y_i(k) = \alpha(k) + \beta[r(k)u_i + (1 - (r(k))^2)^{-.5}w_i(k)]$. Both $x_i(k)$ and $y_i(k)$ have standard deviation β, and their correlation is $r(k)$. A different permutation is used for each scatterplot. The $\alpha(k)$ are chosen so that the center of gravity of the point cloud is at the center of the plotting frame; β has a value that places the extremes of the point cloud for the smallest scale value just inside the plotting frame.
5. F. Mosteller and J. W. Tukey, *Data Analysis and Regression* (Addison-Wesley, Reading, Mass., 1977).
6. P. J. Huber, *Robust Statistics* (Wiley, New York, 1980); F. R. Hampel, *J. Am. Stat. Assoc.* **69**, 383 (1974).
7. J. W. Tukey and D. H. McLaughlin, *Sankhya Ser. A* **25**, 331 (1963).
8. The data for individual subjects generally followed the pattern of the average behavior but was noisier. A few subjects deviated radically, which suggested using 10 percent trimmed means, but the results do not change dramatically if means and their standard errors are used.
9. A referee suggests that the bigger circles in this figure get greater visual weight. This could be investigated by experiments similar to those described here.
10. R. F. Strahan and C. J. Hansen, *Appl. Psychol. Meas.* **2**, 543 (1978); P. Bobko and R. Karren, *Personnel Psychol.* **32**, 313 (1979).
11. D. L. Jennings, T. Amabile, L. Ross, *Judgment Under Uncertainty: Heuristics and Biases*, A. Tversky and D. Kahneman, Eds. (Cambridge Univ. Press, New York, 1980).
12. F. Mosteller, A. F. Siegel, E. Trapido, C. Youtz, *Am. Stat.* **35**, 150 (1981).
13. H. Wainer and D. Thisson, *Appl. Psychol. Meas.* **3**, 543 (1979).
14. M. B. Wilk, *Bell Laboratories Technical Memorandum* (Bell Laboratories, Murray Hill, N.J., 1966).
15. We fit to the data in Fig. 2 a two-parameter family of curves that includes $g(r)$, $w(r)$, r, and r^2. The family is $1 - (1 - r)^\alpha(1 + r)^\beta$. Estimates of the unknown α and β and their standard errors are $.71 \pm .04$ and $.66 \pm .11$, respectively.
16. S. S. Stevens, *Psychophysics: Introduction to Its Perceptual, Neural, and Social Prospects* (Wiley, New York, 1975).
17. P. Tukey, S. Sternberg, and a referee have all pointed out that in the left panel of Fig. 1 the ratio of the plotting-character size relative to the point-cloud size is larger than in the right panel. Perhaps, as the referee has put it, "variables on scatterplots look more highly correlated when the point sizes are increased."
18. We are indebted to R. Gnanadesikan, C. Mallows, S. Sternberg, W. Tapp, P. Tukey, and two referees for helpful comments on our manuscript.

11 December 1981; revised 15 March 1982

Economic Values and Embodied Energy

In his article "Embodied energy and economic valuation" (*1*), Costanza concludes that "With the appropriate boundaries, embodied energy values are accurate indicators of market values where markets exist. . . . they may also be used to determine 'market values' where markets do not exist" and that "the physical dimensions of economic activity are not separable from limitations of energy supply." He uses input-output analysis to support his conclusions and calculates embodied energy as the direct plus indirect energy required to produce goods and services in the U.S. economy.

Costanza makes two major changes in traditional input-output analysis. First, he expands the transaction matrix to include the household and government sectors. With this change, the total net output of the economy is not gross national product (GNP) but the sum of gross capital formation, net inventory change, and net exports. Costanza justifies this shift of system boundaries with Odum's argument (*2*) that primary factors of production (capital, labor, and natural resources) are not independent, but Odum's argument has no bearing on this shift of system boundaries. What this shift of boundaries does mean, for example, is that the household sector receives energy from other sectors in proportion to employee compensation (modified by indirect business taxes and so on). While it is acceptable to argue in a national income accounting sense that the market value of the goods and services received by the household sector is equal to the market value of the employee compensation received (with modification for indirect business taxes and so on), Costanza's tracing of Btu flows in this manner is highly debatable and is, in fact, double counting (although he argues it is not). This shift of system boundaries is the most debatable aspect of Costanza's argument and the most important.

The second major change Costanza makes in traditional input-output analysis is the addition of solar energy flows after correcting for the lower thermodynamic usefulness of direct sunlight in comparison with fossil fuels. He assumes that solar energy enters the economy through the agriculture, forestry, and fisheries sectors according to their relative land areas and admits that this crude approximation should be improved. While it is highly debatable whether solar and environmental services should be valued in terms of non–market-determined Btu flows and added to the market-determined Btu flows of traditional input-output analysis, Costanza's use of solar energy flows has little to do with the conclusions he reached. This in itself may be of interest, since he added a total of 51.5×10^{15} Btu's per year to represent the functional